New Coding Scheme for the State Estimation and Reference Tracking of Nonlinear Dynamic Systems over the Packet Erasure Channel (IoT): Applications in Tele-operation of Autonomous Vehicles

Ali Parsa and Alireza Farhadi

Abstract

This paper presents a new technique for the state estimation and reference tracking of nonlinear dynamic systems over the packet erasure channel, which is an abstract model for transmission via the Internet, WiFi wireless network and ZigBee modules. A new encoder and decoder for real time state estimation of nonlinear dynamic systems at the end of communication link when the measurements are sent through the limited capacity erasure channel, are presented. Then, using the available results from control theory, a controller for reference tracking and hence the stability of the system is also designed. That is, for nonlinear systems, almost sure asymptotic state estimation and reference tracking techniques including an encoder, decoder and a controller are presented. The satisfactory performances of the proposed state estimation and control techniques are illustrated via computer simulations by applying the proposed techniques on the unicycle model, which represents the dynamics of autonomous vehicles.

Keywords- Nonlinear dynamic system, the packet erasure channel, stability, reference tracking, IoT, the unicycle model.

I. Introduction

A. Motivation and Background

In recent years, we are witnessing the exponential growth of the Internet of Things (IoT) in different areas including medical and health care, transportation including the tele-operation of autonomous vehicles, building and home automation, manufacturing, agriculture, energy management, environmental monitoring, etc. This has been facilitated by inventing the ZigBee communication modules. In IoT applications, we deal with the measurement and control of dynamic systems using ZigBee communication modules; or we deal with the measurement and control of dynamic systems over the Internet or WiFi wireless communication networks. This type of communications can be modeled by the packet erasure channel with

A. Parsa was Ph.D. student in the Department of Electrical Engineering at Sharif University of Technology and A. Farhadi is Associate Professor in the Department of Electrical Engineering at Sharif University of Technology (Email: aparsa@alumni.ut.ac.ir; afarhadi@sharif.edu).

This work was supported by the research office of Sharif University of Technology.

feedback acknowledgment. IoT is a fast growing field. This has motivated us to address the problem of measurement and control of nonlinear dynamic systems over the packet erasure channel with applications in the tele-operation of autonomous vehicles. Thus, in this paper we focus on IoT with applications in autonomous vehicles. In recent years, the tele-operation of autonomous vehicles (including drones, road vehicles and under water autonomous vehicles) is also in the sharp attention of research communities due to its vast applications in aerial and under water photography, shipping and delivering, geographical mapping, disaster management, precision agriculture, search and rescue, wildlife monitoring, etc. This has also motivated us to illustrate an application of our theoretical development in the important area of measurement and control of nonlinear dynamic systems over the packet erasure channel in the tele-operation of autonomous vehicles.

Research on real time state estimation at the end of communication links and stability over communication channels subject to imperfections, e.g., limited bit rate, random packet dropout (which is the case in IoT), is concerned with situations involving a dynamic system controlled over a communication link subject to imperfections, as shown in the block diagram of Fig. 1. Fig. 1 illustrates a basic block diagram considered in the literature for studying the problems of state estimation and stability subject to communication imperfections. This basic block diagram has been considered in many research papers (e.g., [1]-[7]). In this block diagram there is a communication link subject to imperfections from sensors to remote controller; while the communication from remote controller to system is perfect. This block diagram can correspond to the tele-operation system of micro autonomous vehicles. As micro autonomous vehicles are subject to limited capacity on - board batteries, the communication from vehicle to remote base station, where the remote controller is located must be performed with minimum possible transmission power in order to increase the life time of the on - board batteries. Therefore, in the block diagram of Fig. 1 the communication from dynamic system to remote controller is subject to communication imperfections (limited bit rate and packet dropout). On the other hand, as the base station can be supplied with high power, the communication from remote controller to dynamic system in the block diagram of Fig. 1 can be assumed to be without imperfections. Thus, in the block diagram of Fig. 1, dynamic system and encoder can have access to control signal. The limitation on transmission capacity (also refereed to as bit rate) results in distortion on measurements that must be compensated by designing proper encoder and decoder for real time reliable data reconstruction of measurements at the end of communication link. Questions of this kind are motivated by future generation of mobile communications, such as 5G and tactile Internet that are explicitly intended to meet latency requirements for control applications [8],[9]. One of the main features of these applications is that the huge numbers of communicating devices are connected through a shared media; and therefore, in these applications information transfer among devices are subject to limited capacity constraint.

In the literature, many works on controlling dynamic systems over the packet erasure channel are concerned with the state estimation and stability of linear dynamic systems over the packet erasure channel (e.g., [1], [2], [10]), in which the transmission of information in addition of random dropout is subject to quantization error imperfection. Over the real erasure channel, in which the transmission of information is only subject to random dropout, the state estimation and/or stability problems of nonlinear dynamic systems have been addressed in a few papers (e.g., [11], [12], [13], [14], [15] [16]). However, few references (e.g., [17], [18]) are concerned with the stability or state estimation of nonlinear dynamic systems over the packet erasure channel. In [18] the problem of reference tracking, stability and state estimation of nonlinear dynamic systems over the packet erasure channel, with applications in the tele-operation of autonomous vehicles, have been addressed by extending the classical linearization method and using linear controllers and a coding scheme for state estimation of linearized systems.

B. Paper Contributions

This paper addresses the problems of state estimation and reference tracking (and hence stability) of nonlinear dynamic systems over the packet erasure channel with feedback acknowledgment, as it is shown by the block diagram of Fig. 1. For the state estimation and reference tracking of the tele-operated system of Fig. 1, which can correspond to the tele-operation system of autonomous vehicles over WiFi or ZigBee, a new nonlinear encoder and decoder for the state estimation of nonlinear dynamic systems by remote controller are presented when measurements are sent through the packet erasure channel subject to random packet dropout and limited bit rate. Then, using the classical control theory tools, a nonlinear controller for reference tracking and hence the stability of the system is designed. That is, for nonlinear dynamic systems, an almost sure asymptotic state estimation and reference tracking techniques including an encoder, decoder and a controller are presented. It is shown that the proposed techniques result in almost sure asymptotic state estimation and reference tracking over the packet erasure channel. The satisfactory performances of the proposed techniques are also illustrated via computer simulations by applying these techniques on the unicycle model, which represents the dynamics of autonomous vehicles. By presenting a new nonlinear coding scheme and controller, this paper extends the previous results on reference tracking, stability and state estimation of nonlinear dynamic systems over the packet erasure channel. In particular, in [18] the same authors have presented a technique for state estimation, reference tracking and stability of nonlinear dynamic systems over the packet erasure channel with applications in tele-operation of autonomous vehicles, where by transmitting with less bits, a better performance can be obtained. However, the technique presented in [18] requires frequent linearization of the nonlinear system and transmission with variable bit rates, where it may not be implementable for some dynamics (e.g., fast dynamics). That is, the proposed nonlinear coding scheme and controller in this paper are implementable with a fixed bit rate to a larger class of nonlinear systems including systems subject to uncertainty.

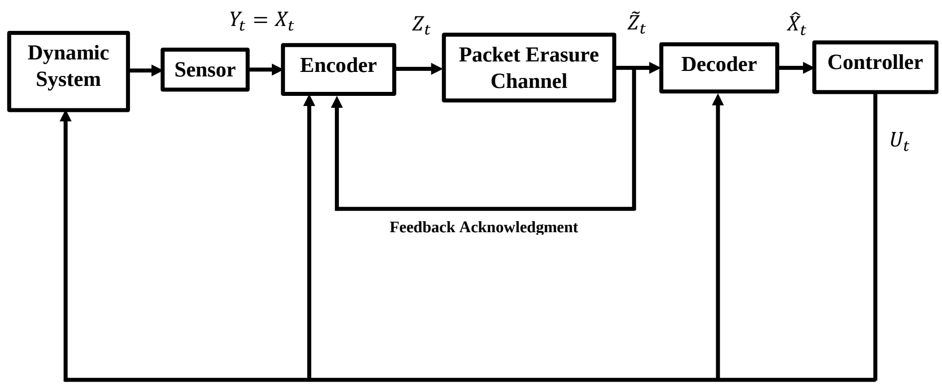

Fig. 1. A dynamic system controlled over the packet erasure channel with feedback acknowledgment

C. Paper Organization

The paper is organized as follows. Section I was devoted to Introduction. In Section II, the problem formulation is presented. Section III is devoted to the design of a proper encoder, decoder and a controller for state estimation and reference tracking of nonlinear dynamic systems over the packet erasure channel. Section IV is devoted to the simulation results for the unicycle model. Finally, the paper is concluded by summarizing the contributions of the paper and direction for future research in Section V.

II. Problem Formulation

Throughout, certain conventions are used: $|\cdot|$ denotes the absolute value, $\|\cdot\|$ the Euclidean norm and V' denotes the transpose of vector/matrix V. A^{-1} and $\det(A)$ denote the inverse and determinant of a square matrix A, respectively. $diag\{\}$ denotes the diagonal matrix. '$\doteq$' means 'by definition is equivalent to' and $Z^t \doteq (Z_1, Z_2, ..., Z_t)$. $\mathbb{R}$ denotes the set of real numbers and $N_+ \doteq \{0, 1, 2, 3, ...\}$. Also, $N(p, q)$ denotes the Gaussian distribution with mean p and covariance q, $\underline{0}$ the zero vector/matrix and I_n denotes n by n identity matrix. $[V]_i$ means the ith element of the vector V.

This paper is concerned with almost sure asymptotic state estimation and reference tracking of nonlinear systems over the packet erasure channel, as is shown in the block diagram of Fig. 1. The building blocks of Fig. 1 are described below:

Dynamic System: The dynamic system is described by the following nonlinear discrete time system:

$$\begin{cases} X_{t+1} = F(X_t) + BU_t \\ Y_t = X_t \end{cases} \tag{1}$$

where $t \in N_+$ is the time instant, $F(X_t) = \begin{bmatrix} f_1(X_t) & f_2(X_t) & ... & f_n(X_t) \end{bmatrix}' \in \mathbb{R}^n$ is a continues nonlinear function, $X_t = \begin{bmatrix} x_t^{(1)} & x_t^{(2)} & ... & x_t^{(n)} \end{bmatrix}' \in \mathbb{R}^n$ is the vector of states of the system, $Y_t \in \mathbb{R}^n$ is the observation signal, $U_t \in \mathbb{R}^q$ is the control signal and $B = \begin{bmatrix} b_1 \\ b_2 \\ . \\ . \\ . \\ b_n \end{bmatrix} \in \mathbb{R}^{n \times q}$, where b_is are the row vectors with the dimension 1 by q. BB' is either invertible or singular. If it is singular, we use the singular value decomposition and pseudo inverse to estimate $B'(BB')^{-1}$, as follows: $BB' = U\Sigma V;\ \Sigma = diag\{\sigma_1, \sigma_2, ..., \sigma_m, 0, ..., 0\},\ m < n \Rightarrow (BB')^{-1} = V^{-1}\Sigma^* U^{-1};\ \Sigma^* = diag\{\frac{1}{\sigma_1}, \frac{1}{\sigma_2}, ..., \frac{1}{\sigma_m}, 0, ..., 0\}$. It is also assumed that $B \neq 0$ and when $F(X_t) = AX_t$, the pair (A, B) is controllable. Throughout, it is assumed that the probability measure associated with the initial state X_0 with components $x_0^{(i)}$, $i = \{1, 2, ..., n\}$, has bounded support. That is, for each $i \in \{1, 2, ..., n\}$ there exists a compact set $[-L_0^{(i)}, L_0^{(i)}] \in \mathbb{R}$ such that $\Pr(x_0^{(i)} \in [-L_0^{(i)}, L_0^{(i)}]) = 1$. Note that X_0 is unknown for decoder and controller ; but it is known for the encoder as the dynamic system is fully observed and the encoder is co-located with the dynamic system and hence it has access to the sensor outputs.

Communication Channel: Communication channel between system and controller is the packet erasure channel with feedback acknowledgment. It is a digital channel that transmits a packet of binary data with the limited R bits length at each channel use. The channel input and output alphabets are denoted by $\mathcal{Z}$ and $\tilde{\mathcal{Z}}$, respectively. Let Z_t denote the channel input at time instant $t \in N_+$, which is a packet of binary data with length R bits containing information bits, also $\tilde{Z}_t$ denote the corresponding channel output. Let also e denote the erasure symbol. Then,

$$\tilde{Z}_t = \begin{cases} Z_t & with\ probability\ 1 - \alpha \\ e & with\ probability\ \alpha \end{cases} \tag{2}$$

That is, this channel erases a transmitted packet with the probability α. Throughout, it is assumed that the erasure probability α is known a priori. In the channel considered in this paper, there are feedback acknowledgments from receiver to encoder. That is, if a transmission is successful, an acknowledgment bit is sent from receiver to encoder indicating that the transmission was successful. The packet erasure channel with feedback acknowledgment is an abstract model for the commonly used data transmission technologies, such as the Internet, WiFi and ZigBee. The capacity of this channel is $(1 - \alpha)R$ bits/time step provided this channel transmits the information about each measurement at each channel use.

To compensate the imperfections on the received measurements which are due to random packet dropout and distortion caused by the limitation on channel capacity, we need to use a proper encoder and decoder. Encoder and decoder considered in this paper have the following general description.

Encoder: Encoder is a causal operator denoted by $Z_t = \mathcal{E}(Y_t, \tilde{Z}^{t-1}, U^{t-1})$ that maps the system output Y_t (by the knowledge of the past channel outputs and control signal) to the channel input Z_t, which is a string of binaries with length R.

Decoder: Decoder is a causal operator denoted by $\hat{X}_t = D(\tilde{Z}^t, U^{t-1})$ that maps the channel outputs to $\hat{X}_t$, which is the estimate of the state variables at decoder.

Controller: Controller has the following structure $U_t = -B'(BB')^{-1}(F(\hat{X}_t) - \mathcal{R}_{t+1})$ where $\mathcal{R}_{t+1}$ is the reference signal. Note that for the stability purposes, we set $\mathcal{R}_{t+1} = \underline{0}$.

The objective of this paper is to design an encoder, decoder and a controller that result in almost sure asymptotic state estimation and reference tracking (and hence stability) of the system (1), as defined below:

Definition 2.1: (Almost Sure Asymptotic State Estimation): Consider the block diagram of Fig. 1 described by the nonlinear dynamic system (1) over the packet erasure channel, as described above. It is said that the states are almost sure asymptotically estimated if there exist an encoder and a decoder such that the following property holds: $\Pr(\lim_{t\to\infty} \|X_t - \hat{X}_t\| = 0) = 1$.

Definition 2.2: (Almost Sure Asymptotic Reference Tracking): Consider the block diagram of Fig. 1 described by the nonlinear dynamic system (1) over the packet erasure channel, as described above. It is said that the system is almost sure asymptotically track the reference signal $\mathcal{R}_t \in \mathbb{R}^n$ if there exist an encoder, decoder and a controller such that the following property holds: $\Pr(\lim_{t\to\infty} \|X_t - \mathcal{R}_t\| = 0) = 1$.

Note that almost sure asymptotic stability is a special case of the reference tracking with $\mathcal{R}_t = \underline{0}$. That is,

Definition 2.3: (Almost Sure Asymptotic Stability): Consider the block diagram of Fig. 1 described by the nonlinear dynamic system (1) over the packet erasure channel, as described above. It is said that the system is almost sure asymptotically stable if there exist an encoder, decoder and a controller such that the following property holds: $\Pr(\lim_{t\to\infty} \|X_t\| = 0) = 1$ for $\mathcal{R}_t = \underline{0}$.

III. Encoder, Decoder and Controller

In this section, we are concerned with the dynamic system (1). We first present an encoder, decoder and a sufficient condition on the length of transmitted packets R, under which the states of the system almost sure asymptotically are estimated at the end of communication link. To achieve this goal and for the simplicity of presentation, we first suppose that $F(X)$ in (1) is strictly monotone and scalar function; then, we generalize the proposed coding scheme to more general form of $F(X)$. Subsequently, we show that using the proposed structure for the controller, the reference tracking and stability are also achieved.

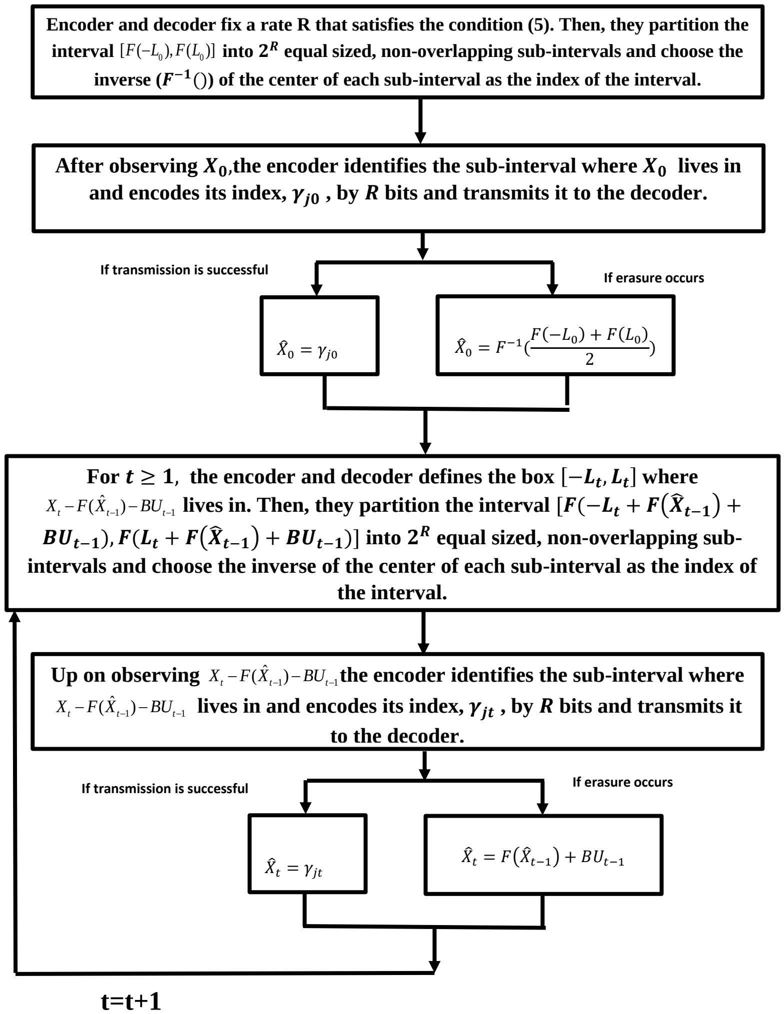

Fig. 2. The proposed coding algorithm for the scalar case

A. Encoder and Decoder: Scalar Case

First, consider the dynamic system (1) with the strictly monotone (e.g., increasing) and scalar function $F(X)$ with continuous first derivative; and suppose that X_t, $U_t \in \mathbb{R}$ $(n, q = 1)$. We present in this section an encoder, a decoder and a sufficient condition on the length of transmitted packets R, under which the states of the system almost sure asymptotically are estimated at the end of communication link. The proposed coding algorithm for the scalar case is depicted in Fig. 2 and it works as follows:

We fix the transmission rate R so that is satisfies the condition (5). At the time instant $t = 0$, we notice that $X_0 \in [-L_0, L_0]$. The encoder and decoder then partition the interval $[F(-L_0), F(L_0)]$ into 2^R equal sized, non-overlapping sub-intervals. Let us denote the center of each sub-interval by $\eta_0, \eta_1, ..., \eta_{2^R-1}$ (see Fig. 3). Then, the projection of η_is in the X-axes is computed and denoted by $\gamma_0 = F^{-1}(\eta_0), \gamma_1 = F^{-1}(\eta_1), ..., \gamma_{2^R-1} = F^{-1}(\eta_{2^R-1})$, where $F^{-1}(.)$ is the inverse function of $F(.)$ (see Fig. 3). Subsequently, the index of the sub-interval that includes X_0 (e.g., γ_{j0} where $j0 \in \{0, 1, ..., 2^R - 1\}$) is encoded into R bits and transmitted to the decoder through the packet erasure channel. If the decoder receives this R bits successfully, it identifies the

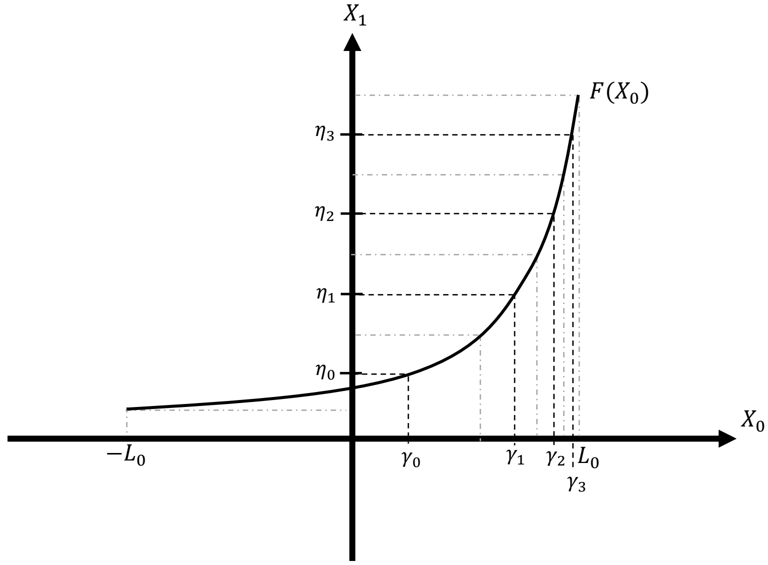

Fig. 3. Equal sized, non-overlapping sub-intervals for encoding with the rate $R = 2$

index of the sub-interval where X_0 lives in; and the value of this index is chosen as $\hat{X}_0$ (e.g., γ_{j0} where $j0 \in \{0, 1, ..., 2^R - 1\}$). But if erasure occurs, then $\hat{X}_0 = F^{-1}(\frac{F(L_0)+F(-L_0)}{2})$. At the time instant $t = 1$, using feedback acknowledgment, the encoder can compute $\hat{X}_0$; and therefore, it encodes $X_1 - F(\hat{X}_0) - BU_0$. To encode this signal, the interval $[-L_1, L_1]$ is computed by the encoder and decoder as follows: Let $\hat{\hat{X}}_1 = F(\hat{X}_0) + BU_0$ be the reconstruction of X_1 at the encoder, then if the packet has been received successfully at the time instant $t = 0$, the decoding error at the encoder is bounded above by $|X_1 - \hat{\hat{X}}_1| = |F(X_0) - F(\hat{X}_0)| \leq \frac{\frac{|F(L_0)-F(-L_0)|}{2}}{2^R}$; and for the other case, $|X_1 - \hat{\hat{X}}_1| = |F(X_0) - F(\hat{X}_0)| \leq \frac{|F(L_0)-F(-L_0)|}{2}$. Hence, $|X_1 - \hat{\hat{X}}_1| = |X_1 - F(\hat{X}_0) - BU_0| = |F(X_0) + BU_0 - F(\hat{X}_0) - BU_0| = |F(X_0) - F(\hat{X}_0)| \leq M_0 \frac{|F(L_0)-F(-L_0)|}{2} \doteq L_1$. Then, similar to the previous case, encoder and decoder partition the interval $[F(-L_1 + F(\hat{X}_0) + BU_0), F(L_1 + F(\hat{X}_0) + BU_0)]$ into 2^R equal sized, non-overlapping sub-intervals and the inverse of the center of each sub-interval is chosen as the index of that interval. When the encoder observes the signal $X_1 - F(\hat{X}_0) - BU_0$, the index of the sub-interval that includes $X_1 - F(\hat{X}_0) - BU_0$ (e.g., γ_{j1} where $j1 \in \{0, 1, ..., 2^R - 1\}$) is encoded into R bits and transmitted to the decoder through the packet erasure channel. Then, the decoder constructs $\hat{X}_1$ as follows:

$$\hat{X}_1 = \begin{cases} \gamma_{j1}, & \Pr(M_1 = \frac{1}{2^R}) = 1 - \alpha \\ F(\hat{X}_0) + BU_0, & \Pr(M_1 = 1) = \alpha \end{cases} \tag{3}$$

Consequently, the decoding error is bounded above by $|X_1 - \hat{X}_1| \leq L_1$. For the time instant $t = 2$, the decoding error at the encoder is bounded above by $|X_2 - \hat{\hat{X}}_2| = |X_2 - F(\hat{X}_1) - BU_1)| = |F(X_1) + BU_1 - F(\hat{X}_1) - BU_1| = |F(X_1) - F(\hat{X}_1)| \leq M_1 \frac{|F(L_1+\Delta_0)-F(-L_1+\Delta_0)|}{2} \doteq L_2$; where $\Delta_0 \doteq F(\hat{X}_0) + BU_0$ and $M_1 = \begin{cases} \frac{1}{2^R}, & \Pr(M_1 = \frac{1}{2^R}) = 1 - \alpha \\ 1, & \Pr(M_1 = 1) = \alpha \end{cases}$.

Similarly, for the rest of time instants $t > 1$, the encoder encodes $X_t - F(\hat{X}_{t-1}) - BU_{t-1}$. To encode this signal, the interval $[-L_t, L_t]$ is chosen as follows:$|X_t - \hat{\hat{X}}_t| = |X_t - F(\hat{X}_{t-1}) - BU_{t-1})| = |F(X_{t-1}) + BU_{t-1} - F(\hat{X}_{t-1}) - BU_{t-1}| = |F(X_{t-1}) - F(\hat{X}_{t-1})| \leq M_{t-1}\frac{|F(L_{t-1}+\Delta_{t-2})-F(-L_{t-1}+\Delta_{t-2})|}{2} \doteq L_t; M_{t-1} = \begin{cases} \frac{1}{2^R}, & \Pr(M_{t-1} = \frac{1}{2^R}) = 1-\alpha \\ 1, & \Pr(M_{t-1} = 1) = \alpha \end{cases}$ where $\Delta_{t-2} \doteq F(\hat{X}_{t-2}) + BU_{t-2}$.

Then, the encoder and decoder partition the interval $[F(-L_t + F(\hat{X}_{t-1}) + BU_{t-1}), F(L_t + F(\hat{X}_{t-1}) + BU_{t-1})]$ into 2^R equal sized, non-overlapping sub-intervals and the inverse of the center of each sub-interval is chosen as the index of that interval. When the encoder observes the signal $X_t - F(\hat{X}_{t-1}) - BU_{t-1}$, the index of the sub-interval that includes $X_t - F(\hat{X}_{t-1}) - BU_{t-1}$ (e.g., γ_{jt}) is encoded into R bits and transmitted to the decoder through the packet erasure channel. Then the decoder constructs $\hat{X}_t$ as below:

$$\hat{X}_t = \begin{cases} \gamma_{jt}, & \Pr(M_{t-1} = \frac{1}{2^R}) = 1-\alpha \\ F(\hat{X}_{t-1}) + BU_{t-1}, & \Pr(M_{t-1} = 1) = \alpha \end{cases} \tag{4}$$

Consequently, the decoding error is bounded above by $|X_t - \hat{X}_t| \leq L_t$. By following a similar procedure, as described above, the sequence $\hat{X}_0, \hat{X}_1, \hat{X}_2, \ldots$ are constructed at the decoder.

Let $\Gamma_{Max} \doteq \max_{X,Y\in\mathcal{D}} \frac{|F(X)-F(Y)|}{|X-Y|}$, where $\mathcal{D}$ is the domain of the system; and $\Gamma_t \doteq \frac{|F(L_t+F(\hat{X}_{t-1})+BU_{t-1})-F(-L_t+F(\hat{X}_{t-1})+BU_{t-1})|}{2L_t}$. Now, we must show that the above coding scheme results in almost sure asymptotic state estimation. This result is shown in the following proposition.

Proposition 3.1: Consider the control system of Fig. 1 described by the dynamic system (1) over the packet erasure channel with erasure probability α and feedback acknowledgment, as described earlier. Suppose that the scalar function $F(X)$ in the dynamic system (1) is strictly monotone function with continuous first derivative. Also, suppose that the transmission rate R satisfies the following inequality:

$$(1-\alpha)R > \max\{0, \log_2 \Gamma_{Max}\} \tag{5}$$

Then, using the proposed encoding and decoding scheme, we have almost sure asymptotic state estimation in the form of $\hat{X}_t \to X_t$, P-a.s.; or equivalently, $\Pr(\lim_{t\to\infty} \|X_t - \hat{X}_t\| = 0) = 1$.

Proof: : Choose any rate R that satisfies the condition (5). For this rate, define the random variable M_t as follows:

$$M_t = \begin{cases} \frac{1}{2^R}, & \Pr(M_t = \frac{1}{2^R}) = 1-\alpha \\ 1, & \Pr(M_t = 1) = \alpha \end{cases} \tag{6}$$

This random variable is the indicator of successful transmission or failed transmission at time instant t. Using the above encoding and decoding scheme, we have $|X_0 - \hat{X}_0| \leq L_0$, $|X_1 - \hat{X}_1| \leq M_0\frac{|F(L_0)-F(-L_0)|}{2} = L_1 = M_0\Gamma_0 L_0 \leq M_0\Gamma_{Max}L_0$, $|X_2 - \hat{X}_2| \leq M_1\frac{|F(L_1+\Delta_0)-F(-L_1+\Delta_0)|}{2} = L_2 = M_1\Gamma_1 L_1 \leq M_1 M_0 \Gamma_{Max}^2 L_0, \ldots, |X_t - \hat{X}_t| \leq M_{t-1}\frac{|F(L_{t-1}+\Delta_{t-2})-F(-L_{t-1}+\Delta_{t-2})|}{2} =$

$L_t = M_{t-1}\Gamma_{t-1}L_{t-1} \leq ... \leq M_{t-1}...M_1M_0\Gamma_{Max}^t L_0$. Therefore, $|X_t - \hat{X}_t| \leq M_{t-1}...M_1M_0\Gamma_{Max}^t L_0 = L_0\prod_{i=0}^{t-1} M_i\Gamma_{Max} = L_0(2^{\log_2(\prod_{i=0}^{t-1} M_i\Gamma_{Max})}) = 2^{t(\frac{1}{t}\sum_{i=0}^{t-1}\log_2(M_i\Gamma_{Max}))}$.

Since M_i is an i.i.d. sequence and $E[M_i] < \infty$ for each i, when $t \to \infty$, from the strong law of large numbers [19] we have: $\frac{1}{t}\sum_{i=0}^{t-1}\log_2(M_i\Gamma_{Max})) \to E[\log_2(M_i\Gamma_{Max})] = (1-\alpha)\log_2(\frac{1}{2^R}\Gamma_{Max}) + \alpha\log_2(\Gamma_{Max})$. Now, as the rate R was chosen so that $(1-\alpha)R > \max\{0, \log_2\Gamma_{Max}\}$, the following inequality holds $(1-\alpha)\log_2(\frac{1}{2^R}\Gamma_{Max}) + \alpha\log_2(\Gamma_{Max}) < 0$. Hence, $\hat{X}_t \to X_t$ as $t \to \infty$, P-a.s. This completes the proof for the monotone scalar case.

B. Encoder and Decoder: Vector Case

Now, consider the dynamic system (1) with the strictly monotone function $f_i(X)$, with continuous first derivatives and suppose that $X_t \in \mathbb{R}^n$ and $U_t \in \mathbb{R}^m$. $f_i(X)$ is a strictly monotone function of X, which means that it is strictly increasing/decreasing with respect to each component of X whenever the others are fixed. At the time instant $t = 0$, we notice that the initial state is X_0 with the components $x_0^{(i)}$, $i = \{1, 2, ..., n\}$ (recall that for each $i \in \{1, 2, ..., n\}$ there exists a compact set $[-L_0^{(i)}, L_0^{(i)}] \in \mathbb{R}$ such that $\Pr(x_0^{(i)} \in [-L_0^{(i)}, L_0^{(i)}]) = 1$); and the rate is $R \doteq \sum_{i=1}^n R^{(i)}$. At each time instant $t \in N_+$ the encoder and decoder partition the intervals $[f_i(\mathbf{m}_t^{[i]}), f_i(\mathbf{M}_t^{[i]})]$ (in $f_i(X)$ axis), where $\mathbf{m}_t^{[i]} \doteq \arg\min_{x^{(j)} \in [-L_t^{(j)}, L_t^{(j)}] \;\&\; x^{(i)} = -L_t^{(i)}} f_i(X)$ and $\mathbf{M}_t^{[i]} \doteq \arg\max_{x^{(j)} \in [-L_t^{(j)}, L_t^{(j)}] \;\&\; x^{(i)} = L_t^{(i)}} f_i(X)$; $\forall t \in N_+,\ i \in \{1, 2, ..., n\}$ and $j \in \{1, 2, ..., i-1, i+1, ..., n\}$ into $2^{R^{(i)}}$ equal sized, non-overlapping sub-intervals and the center of each sub-interval is denoted by $\eta_0^{(i)}, \eta_1^{(i)}, ..., \eta_{2^{R^{(i)}}-1}^{(i)}$. Then, in the corresponding $x_0^{(i)}$ - axis, the corresponding index i is computed as $\gamma_0^{(i)} = {f_{i,m}}^{-1}(\eta_0^{(i)})$,

$\gamma_1^{(i)} = {f_{i,m}}^{-1}(\eta_1^{(i)}), ..., \gamma_{(2^{R^{(i)}-1})-1}^{(i)} = {f_{i,m}}^{-1}(\eta_{(2^{R^{(i)}-1})-1}^{(i)}), \gamma_{2^{(R^{(i)}-1)}}^{(i)} = {f_{i,M}}^{-1}(\eta_{2^{(R^{(i)}-1)}}^{(i)}), ..., \gamma_{(2^{R^{(i)}})-1}^{(i)}$

$= {f_{i,M}}^{-1}(\eta_{(2^{R^{(i)}})-1}^{(i)})$; where ${f_{i,m}}^{-1}(g_i) \doteq {f_i}^{-1}(g_i \mid {x_t}^{(j)} = {\mathbf{m}_t^{[i]}}^{(j)};\ \forall j \in \{1, 2, ..., i-1, i+1, ..., n\})$ (${\mathbf{m}_t^{[i]}}^{(j)}$ is the jth element of the vector $\mathbf{m}_t^{[i]}$) and ${f_{i,M}}^{-1}(g_i) \doteq {f_i}^{-1}(g_i \mid {x_t}^{(j)} = {\mathbf{M}_t^{[i]}}^{(j)};\ \forall j \in \{1, 2, ..., i-1, i+1, ..., n\})$ (${\mathbf{M}_t^{[i]}}^{(j)}$ is the jth element of the vector $\mathbf{M}_t^{[i]}$) which we call them the special inverse functions of $g_i = f_i(X_t)$. Subsequently, the index of the sub-interval that includes $x_0^{(i)}$ (e.g., $\gamma_{j0}^{(i)}$ where $j0 \in \{0, 1, ..., (2^{R^{(i)}-1}) - 1, 2^{R^{(i)}-1}, ..., (2^{R^{(i)}}) - 1\}$) is encoded into $R^{(i)}$ bits and transmitted to the decoder through the packet erasure channel. If the decoder receives this $R^{(i)}$ bits successfully, it identifies the index of the sub-interval where $x_0^{(i)}$ lives in; and the value of this index is chosen as $\hat{x}_0^{(i)}$ (e.g., $\gamma_{j0}^{(i)}$ where $j0 \in \{0, 1, ..., 2^{R^{(i)}} - 1\}$). Otherwise, $\hat{x}_0^{(i)} = [f_i^{-1}(\frac{f_i(\mathbf{M}_0^{[i]}) + f_i(\mathbf{m}_0^{[i]})}{2})]_i$. At the time instant $t = 1$, using feedback acknowledgment, the encoder can compute $\hat{X}_0$; and therefore, it encodes $x_1^{(i)} - f_i(\hat{X}_0) - b_iU_0$. To encode this signal, the interval $[-L_1^{(i)}, L_1^{(i)}]$ is computed by the encoder and decoder as follows: Let $\hat{\hat{x}}_1^{(i)} = f_i(\hat{X}_0) + b_iU_0$ be the reconstruction of $x_1^{(i)}$ at the encoder. Then, if the packet has been received successfully at time instant $t = 0$, the decoding error at the encoder is bounded above by $|x_1^{(i)} - \hat{\hat{x}}_1^{(i)}| = |f_i(X_0) - f_i(\hat{X}_0)| \leq \frac{\frac{|f_i(\mathbf{M}_0^{[i]}) - f_i(\mathbf{m}_0^{[i]})|}{2}}{2^{R^{(i)}}}$; and for the other case is bounded above by $|x_1^{(i)} - \hat{\hat{x}}_1^{(i)}| = |f_i(X_0) - f_i(\hat{X}_0)| \leq \frac{|f_i(\mathbf{M}_0^{[i]}) - f_i(\mathbf{m}_0^{[i]})|}{2}$. Hence,

$$|x_1^{(i)}-\hat{\hat{x}}_1^{(i)}|=|x_1^{(i)}-f_i(\hat{X}_0)-b_iU_0|=|f_i(X_0)+b_iU_0-f_i(\hat{X}_0)-b_iU_0|=|f_i(X_0)-f_i(\hat{X}_0)|\leq M_0^{(i)}\frac{|f_i(\mathbf{M}_0^{[i]})-f_i(\mathbf{m}_0^{[i]})|}{2}\doteq L_1^{(i)} \tag{7}$$

Then similar to the previous case, encoder and decoder partition the interval $[f_i(\mathbf{m}_1^{[i]}+F(\hat{X}_0)+BU_0), f_i(\mathbf{M}_1^{[i]}+F(\hat{X}_0)+BU_0)]$ into $2^{R^{(i)}}$ equal sized, non-overlapping sub-intervals and the special inverse function (i.e., ${f_{i,m}}^{-1}(.)$ and ${f_{i,M}}^{-1}(.)$) of the center of each sub-interval is chosen as the index of that interval. When the encoder observes the signal $x_1^{(i)}-f_i(\hat{X}_0)-b_iU_0$, the index of the sub-interval that includes $x_1^{(i)}-f_i(\hat{X}_0)-b_iU_0$ (e.g., $\gamma_{j1}^{(i)}$ where $j1\in\{0,1,...,2^{R^{(i)}}-1\}$) is encoded into $R^{(i)}$ bits and transmitted to the decoder through the packet erasure channel. Then, the decoder constructs $\hat{x}_1^{(i)}$ as follows:

$$\hat{x}_1^{(i)}=\begin{cases}\gamma_{j1}^{(i)}, & \Pr(M_1^{(i)}=\frac{1}{2^{R^{(i)}}})=1-\alpha\\ f_i(\hat{X}_0)+b_iU_0, & \Pr(M_1^{(i)}=1)=\alpha\end{cases} \tag{8}$$

Consequently, for this case the decoding error is bounded above by $|x_1^{(i)}-\hat{x}_1^{(i)}|\leq L_1^{(i)}$. For the time instant $t=2$, the decoding error at the encoder is bounded above by

$$\begin{aligned}&|x_2^{(i)}-\hat{\hat{x}}_2^{(i)}|=|x_2^{(i)}-f_i(\hat{X}_1)-b_iU_1)|=|f_i(X_1)+b_iU_1-f_i(\hat{X}_1)-b_iU_1|=|f_i(X_1)-f_i(\hat{X}_1)|\\&\leq M_1^{(i)}\frac{|f_i(\mathbf{M}_1^{[i]}+\Delta_0)-f_i(\mathbf{m}_1^{[i]}+\Delta_0)|}{2}\doteq L_2^{(i)};M_1^{(i)}=\begin{cases}\frac{1}{2^{R^{(i)}}}, & \Pr(M_1^{(i)}=\frac{1}{2^{R^{(i)}}})=1-\alpha\\ 1, & \Pr(M_1^{(i)}=1)=\alpha\end{cases}\end{aligned} \tag{9}$$

where $\Delta_0\doteq F(\hat{X}_0)+BU_0$.

Similarly, for the rest of time instants $t>1$, the encoder encodes $x_t^{(i)}-f_i(\hat{X}_{t-1})-b_iU_{t-1}$. To encode this signal the interval $[-L_t^{(i)},L_t^{(i)}]$ is chosen as follows:

$$\begin{aligned}&|x_t^{(i)}-\hat{\hat{x}}_t^{(i)}|=|x_t^{(i)}-f_i(\hat{X}_{t-1})-b_iU_{t-1})|=|f_i(X_{t-1})+b_iU_{t-1}-f_i(\hat{X}_{t-1})-b_iU_{t-1}|=|f_i(X_{t-1})-f_i(\hat{X}_{t-1})|\\&\leq M_{t-1}^{(i)}\frac{|f_i(\mathbf{M}_{t-1}^{[i]}+\Delta_{t-2})-f_i(\mathbf{m}_{t-1}^{[i]}+\Delta_{t-2})|}{2}\doteq L_t^{(i)};M_{t-1}^{(i)}=\begin{cases}\frac{1}{2^{R^{(i)}}}, & \Pr(M_{t-1}^{(i)}=\frac{1}{2^{R^{(i)}}})=1-\alpha\\ 1, & \Pr(M_{t-1}^{(i)}=1)=\alpha\end{cases}\end{aligned} \tag{10}$$

where $\Delta_{t-2}\doteq F(\hat{X}_{t-2})+BU_{t-2}$.

Then, the encoder and decoder partition the interval $[f_i(\mathbf{m}_t^{[i]}+F(\hat{X}_{t-1})+BU_{t-1}), f_i(\mathbf{M}_t^{[i]}+F(\hat{X}_{t-1})+BU_{t-1})]$ into $2^{R^{(i)}}$ equal sized, non-overlapping sub-intervals and the inverse of the center of each sub-interval is chosen as the index of that interval. When the encoder observes the signal $x_t^{(i)}-f_i(\hat{X}_{t-1})-b_iU_{t-1}$, the index of the sub-interval that includes $x_t^{(i)}-f_i(\hat{X}_{t-1})-b_iU_{t-1}$ (e.g., $\gamma_{jt}^{(i)}$) is encoded into $R^{(i)}$ bits and transmitted to the decoder through the packet erasure channel. Then the decoder constructs $\hat{X}_t$ as follows:

$$\hat{x}_t^{(i)} = \begin{cases} \gamma_{jt}^{(i)}, & \Pr(M_{t-1}^{(i)} = \frac{1}{2^{R^{(i)}}}) = 1-\alpha \\ f_i(\hat{X}_{t-1}) + b_i U_{t-1}, & \Pr(M_{t-1}^{(i)} = 1) = \alpha \end{cases} \tag{11}$$

Consequently, the decoding error is bounded above by $|x_t^{(i)} - \hat{x}_t^{(i)}| \le L_t^{(i)}$. By following a similar procedure, as described above, the sequence $\hat{X}_0, \hat{X}_1, \hat{X}_2, ...$ are constructed at the decoder. Let

$$\Gamma_{Max}^{(i)} \doteq \max_{x^{(i)}, y^{(i)} \in \mathcal{D}^{(i)};\ \forall i \in \{1,2,\ldots,n\}} \frac{|f_i(X) - f_i(Y)|}{|x^{(i)} - y^{(i)}|},$$

where $\mathcal{D}^{(i)}$ is the domain of the ith system; and

$$\Gamma_t^{(i)} \doteq \frac{|f_i(\mathbf{M}_t^{[i]} + \Delta_{t-1}) - f_i(\mathbf{m}_t^{[i]} + \Delta_{t-1})|}{2L_t^{(i)}}$$

where $Y = \begin{bmatrix} y^{(1)} & y^{(2)} & ... & y^{(n)} \end{bmatrix}'$ and $\Delta_{t-1} \doteq F(\hat{X}_{t-1}) + BU_{t-1}$.

Now, we must show that the above coding scheme results in almost sure asymptotic state estimation. This result is shown in the following proposition.

Proposition 3.2: Consider the system of Fig. 1 described by the dynamic system (1) over the packet erasure channel with erasure probability α and feedback acknowledgment, as described earlier. Suppose that the nonlinear function $f_i(X)$ is strictly monotone function with continuous first derivatives. Also, suppose that the transmission rate $R = \sum_{i=1}^{n} R^{(i)}$ satisfies the following inequality:

$$(1-\alpha)R^{(i)} > \max\{0, \log_2 \Gamma_{Max}^{(i)}\} \tag{12}$$

Then, using the proposed encoding and decoding scheme, we have almost sure asymptotic state estimation in the form of $\hat{X}_t \to X_t$, P-a.s.; or equivalently, $\Pr(\lim_{t\to\infty} \|X_t - \hat{X}_t\| = 0) = 1$.

Proof: : Choose any rate $R^{(i)}$ that satisfies the condition (12). For this rate, define the random variable $M_t^{(i)}$ as follows:

$$M_t^{(i)} = \begin{cases} \frac{1}{2^{R^{(i)}}}, & \Pr(M_t^{(i)} = \frac{1}{2^{R^{(i)}}}) = 1-\alpha \\ 1, & \Pr(M_t^{(i)} = 1) = \alpha \end{cases} \tag{13}$$

This random variable is the indicator of successful transmission or failed transmission at time instant t. Using the above encoding and decoding scheme, we have

$$|x_0^{(i)} - \hat{x}_0^{(i)}| \le L_0^{(i)}$$

$$|x_1^{(i)} - \hat{x}_1^{(i)}| \le M_0^{(i)} \frac{|f_i(\mathbf{M}_0^{[i]}) - f_i(\mathbf{m}_0^{[i]})|}{2} = L_1^{(i)} = M_0^{(i)} \Gamma_0^{(i)} L_0^{(i)} \le M_0^{(i)} \Gamma_{Max}^{(i)} L_0^{(i)}$$

$$|x_2^{(i)} - \hat{x}_2^{(i)}| \leq M_1^{(i)} \frac{|f_i(\mathbf{M}_1^{[i]} + \Delta_0^{(i)}) - f_i(\mathbf{m}_1^{[i]} + \Delta_0^{(i)})|}{2} = L_2^{(i)} = M_1^{(i)} \Gamma_1^{(i)} L_1^{(i)} \leq M_1^{(i)} M_0^{(i)} {\Gamma_{Max}^{(i)}}^2 L_0^{(i)}$$

$$\vdots$$

$$|x_t^{(i)} - \hat{x}_t^{(i)}| \leq M_{t-1}^{(i)} \frac{|f_i(\mathbf{M}_{t-1}^{[i]} + \Delta_{t-2}) - f_i(\mathbf{m}_{t-1}^{[i]} + \Delta_{t-2})|}{2} = L_t^{(i)} = M_{t-1}^{(i)} \Gamma_{t-1}^{(i)} L_{t-1}^{(i)} \leq ... \leq M_{t-1}^{(i)} ... M_1^{(i)} M_0^{(i)} {\Gamma_{Max}^{(i)}}^t L_0^{(i)}$$

$$\vdots \tag{14}$$

Therefore,

$$\begin{aligned} |x_t^{(i)} - \hat{x}_t^{(i)}| &\leq M_{t-1}^{(i)} ... M_1^{(i)} M_0^{(i)} {\Gamma_{Max}^{(i)}}^t L_0^{(i)} \\ &= L_0^{(i)} \prod_{j=0}^{t-1} M_j^{(i)} \Gamma_{Max}^{(i)} = L_0^{(i)} (2^{\log_2(\prod_{j=0}^{t-1} M_j^{(i)} \Gamma_{Max}^{(i)})}) = 2^{t(\frac{1}{t} \sum_{j=0}^{t-1} \log_2(M_j^{(i)} \Gamma_{Max}^{(i)}))} \end{aligned} \tag{15}$$

Now, as $M_j^{(i)}$ is an i.i.d. sequence and $E[M_j^{(i)}] < \infty$ for each i and j, as $t \to \infty$, from the strong law of large numbers [19] we have:

$$\frac{1}{t} \sum_{j=0}^{t-1} \log_2(M_j^{(i)} \Gamma_{Max}^{(i)})) \to E[\log_2(M_j^{(i)} \Gamma_{Max}^{(i)})] = (1 - \alpha) \log_2(\frac{1}{2^{R^{(i)}}} \Gamma_{Max}^{(i)}) + \alpha \log_2(\Gamma_{Max}^{(i)}) \tag{16}$$

Now, as the rate $R^{(i)}$ was chosen so that

$$(1 - \alpha) R^{(i)} > \max\{0, \log_2 \Gamma_{Max}^{(i)}\}, \tag{17}$$

the following inequality holds

$$(1 - \alpha) \log_2(\frac{1}{2^{R^{(i)}}} \Gamma_{Max}^{(i)}) + \alpha \log_2(\Gamma_{Max}^{(i)}) < 0. \tag{18}$$

That is, from (15) and (16), $\hat{X}_t \to X_t$ as $t \to \infty$, P-a.s. This completes the proof.

Remark 3.3: For the linear case with the distinct eigenvalues, where $F(X) = AX$ in the system (1), the above sufficient condition reduces to the eigenvalues rate condition, which is the tight bound for almost sure stability of linear systems [1].

Proof: Without loss of generality, suppose that the system matrix A is in the real Jordan form. This form is obtained by implementing a proper similarity transformation; and as a result of that, the linear dynamic system is decomposed into several decoupled sub-systems (i.e., $f_i(X) = \lambda_i x^{(i)}$, where λ_i is the ith distinct eigenvalue of the system matrix A). Therefore,

$$\begin{aligned} \Gamma_{Max}^{(i)} &= \max_{x^{(i)}, y^{(i)} \in \mathcal{D}^{(i)};\ \forall i \in \{1,2,...,n\}} \frac{|f_i(X) - f_i(Y)|}{|x^{(i)} - y^{(i)}|} = \max_{x^{(i)}, y^{(i)} \in \mathcal{D}^{(i)};\ \forall i \in \{1,2,...,n\}} \frac{|\lambda_i x^{(i)} - \lambda_i y^{(i)}|}{|x^{(i)} - y^{(i)}|} \\ &= \max_{x^{(i)}, y^{(i)} \in \mathcal{D}^{(i)};\ \forall i \in \{1,2,...,n\}} \frac{|\lambda_i| |x^{(i)} - y^{(i)}|}{|x^{(i)} - y^{(i)}|} = |\lambda_i|. \end{aligned} \tag{19}$$

Therefore, the eigenvalues rate condition is achieved.

C. Controller

Now, in the following proposition, we show that the proposed coding scheme combined with the controller $U_t = -B'(BB')^{-1}(F(\hat{X}_t) - \mathcal{R}_{t+1})$ result in the reference tracking.

Proposition 3.4: Suppose that the aforementioned assumptions on the matrix B holds. Then, the proposed coding scheme combined with the controller $U_t = -B'(BB')^{-1}(F(\hat{X}_t) - \mathcal{R}_{t+1})$ results in almost sure reference tracking of the system.

Proof: From (1) we have $X_{t+1} = F(X_t) - BB'(BB')^{-1}(F(\hat{X}_t) - \mathcal{R}_{t+1})) = F(X_t) - F(\hat{X}_t) + \mathcal{R}_{t+1}$. Now, using the proposed encoding and decoding scheme, we have $\hat{X}_t \to X_t$ for $t \to \infty$, P-a.s.; and hence, $F(X_t) - F(\hat{X}_t) + \mathcal{R}_{t+1} \to \mathcal{R}_{t+1}$, P-a.s. That is, the reference tracking (and hence stability for the case of $\mathcal{R}_{t+1} = \underline{0}$) is achieved.

IV. Simulation Results

In this section, for the purpose of illustration, we apply the proposed encoder, decoder and controller to the nonlinear dynamics of the miniature drones, autonomous road vehicles and autonomous under water vehicles that can be modeled by the unicycle model [11]. The dynamics of miniature drones, autonomous road vehicles and autonomous under water vehicles are described by a 6 degrees of freedom model. However, the vehicles dynamic can be handled by local control loops, which results in a kinematic unicycle model, as follows [11]:

$$\begin{cases} \dot{x}(t) = v(t)\cos(\phi(t)) \\ \dot{y}(t) = v(t)\sin(\phi(t)) \\ \dot{\phi}(t) = u(t) \end{cases} \tag{20}$$

where $x(t)$, $y(t)$ are the position vector, $\phi(t)$ the heading angle, and the control inputs are the vehicle forward velocity $v(t)$ and the turning rate $u(t)$. The state vector of the system is $X(t) = \begin{bmatrix} x(t) & y(t) & \phi(t) \end{bmatrix}'$ and the input vector is $U(t) = u(t)$, as for the simulations study we fix $v(t) = 1$. The discrete time equivalent model is described by (21), where T is the sampling period.

$$\begin{cases} x_{t+1} = x_t + Tv_t\cos(\phi_t) \\ y_{t+1} = y_t + Tv_t\sin(\phi_t) \\ \phi_{t+1} = \phi_t + Tu_t \end{cases} \tag{21}$$

In this model x_t, y_t, ϕ_t, v_t and u_t are the discrete time equivalent signals of $x(t)$, $y(t)$, $\phi(t)$, $v(t)$ and $u(t)$, respectively. Note that for this model, the state vector is $X_t = \begin{bmatrix} x_t & y_t & \phi_t \end{bmatrix}' \doteq \begin{bmatrix} x_t^{(1)} & x_t^{(2)} & x_t^{(3)} \end{bmatrix}'$.

Therefore, the state space representation of the equivalent discrete time system has the following form:

$$\begin{bmatrix} x_{t+1} \\ y_{t+1} \\ \phi_{t+1} \end{bmatrix} = \begin{bmatrix} x_t + Tv_t \cos(\phi_t) \\ y_t + Tv_t \sin(\phi_t) \\ \phi_t \end{bmatrix} + \begin{bmatrix} 0 \\ 0 \\ T \end{bmatrix} u_t \tag{22}$$

which is in the form of the system (1) with $F(X_t) = \begin{bmatrix} x_t + Tv_t \cos(\phi_t) & y_t + Tv_t \sin(\phi_t) & \phi_t \end{bmatrix}' \doteq \begin{bmatrix} f_1(X_t) & f_2(X_t) & f_3(X_t) \end{bmatrix}'$ and $B = \begin{bmatrix} 0 \\ 0 \\ T \end{bmatrix}$. The autonomous vehicle must track a circle with the center located at (x_r, y_r) and the radius of ρ with the angular velocity of ω_r. Therefore, $\begin{bmatrix} x_t & y_t & \phi_t \end{bmatrix}'$ must track the reference signal $\begin{bmatrix} r_t^{[x]} & r_t^{[y]} & r_t^{[\phi]} \end{bmatrix}'$, where $r_x(t) = x_r + \rho\cos(\omega_r Tt)$, $r_t^{[y]} = y_r + \rho\sin(\omega_r Tt)$ and $r_t^{[\phi]} = \arctan(\frac{r_t^{[y]} - y_{t-1}}{r_t^{[x]} - x_{t-1}})$ (see Fig. 4). Note that for the simplicity of the design, we choose the forward velocity constant and equals to $v(t) = 1\ m/s$. Therefore, for tracking a circle with the center located at $(2, 1)$ and the radius of 2, by the autonomous vehicle, we choose

$$\mathcal{R}_t(X_t) \doteq \begin{bmatrix} r_t^{[x]} & r_t^{[y]} & r_t^{[\phi]} \end{bmatrix}' =$$
$$\begin{bmatrix} 2 + 2\cos(0.5T\ t) & 1 + 2\sin(0.5T\ t) & \arctan(\frac{r_t^{[y]} - y_{t-1}}{r_t^{[x]} - x_{t-1}}) \end{bmatrix}'$$

as the reference signals. For simulations, we also choose $T = 0.01\,\text{sec}$, $x_0,\ y_0 \in [-10, 10]$, $\phi_0 \in [-\frac{\pi}{2}, \frac{\pi}{2}]$ and $\alpha = 0.9$, which indicates that 90 percent of the transmitted packets are dropped. Also, for designing the controller, we use $u_t = -B'(BB')^{-1}(F(\hat{X}_t) - \mathcal{R}_{t+1}(\hat{X}_{t+1}))$, where $\mathcal{R}_t(\hat{X}_t) \doteq \begin{bmatrix} 2 + 2\cos(0.5T\ t) & 1 + 2\sin(0.5T\ t) & \arctan(\frac{r_t^{[y]} - \hat{y}_{t-1}}{r_t^{[x]} - \hat{x}_{t-1}}) \end{bmatrix}'$. By computing the pseudo inverse of B using its singular values, we get $B'(BB')^{-1} = [0 \quad 0 \quad T^{-1}]$ and therefore $u_t = -T^{-1}(\hat{\phi}_t - \arctan(\frac{r_{t+1}^{[y]} - \hat{y}_t}{r_{t+1}^{[x]} - \hat{x}_t}))$. Fig. 5 to Fig. 9 illustrate the results of the simulations. They illustrate that the desired tracking is achieved although 90 percent of transmitted packets are dropped. Table I shows the transmission rates $R^{(i)}$, $i = 1, 2, 3$, used in order to have a satisfactory simulation for different values for α's: $\alpha = 0.5$, $\alpha = 0.9$ and $\alpha = 0.95$. All of these rates satisfy the condition (12) of the main Proposition 3.2. Note that for the conditions simulated $\Gamma_{Max}^{(1)} = 2$, $\Gamma_{Max}^{(2)} = 2$ and $\Gamma_{Max}^{(3)} = \pi$ and for each α the corresponding rates $R^{(i)}$ have been chosen so that $R^{(i)}$ is the smallest integer greater than $\frac{1}{1-\alpha}\max\{0, \Gamma_{Max}^{(i)}\}$. As it is clear from Table I, for α's that are very close to one, reliable real time state estimation and subsequently a satisfactory reference tracking performance using the proposed techniques in this paper are still possible but by allocating very large transmission rates; and as α converges to one, the rates that result in a satisfactory performance significantly rise.

Now, to make simulations study more interesting, we suppose that the nonlinear dynamic system (22) is subject to the

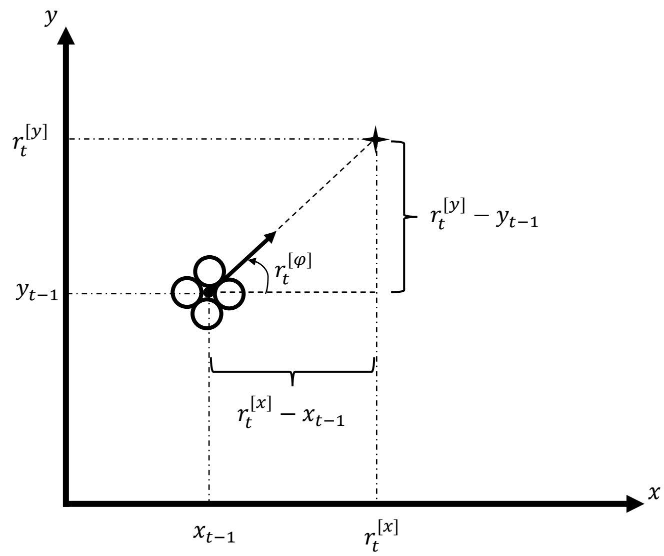

Fig. 4. An autonomous vehicle with the positions x_{t-1} and y_{t-1} moving toward the desired positions $r_t^{[x]}$ and $r_t^{[y]}$, respectively

TABLE I

THE RATES $R^{(i)}$'S USED FOR A SATISFACTORY SIMULATION FOR DIFFERENT α'S.

i	$\alpha = 0.5, R^{(i)}$	$\alpha = 0.9, R^{(i)}$	$\alpha = 0.95, R^{(i)}$
1	3	11	21
2	3	11	21
3	4	17	34

i.i.d. process noise of $W_t \sim N(\underline{0}, I_3)$; while the encoder, decoder and controller are unaware of this process noise. The Root Sum Square Error (RSSE) computed from the sample t = 30/T to the sample t = 50/T (30 sec. to 50 sec.) for $\alpha = 0.5$, $\alpha = 0.9$ and $\alpha = 0.95$ for the case of without process noise and with the above process noise have been reported in Table II. Note that the RSSE from the sample $t = 30/T$ to the sample $t = 50/T$ is defined as $RSSE = \sqrt{\sum_{t=30/T}^{50/T}(x_t - r_t^{[x]})^2 + (y_t - r_t^{[y]})^2 + (\phi_t - r_t^{[\phi]})^2}$. Fig. 10 also illustrates the performance of the proposed technique in the presence of the process noise for $\alpha = 0.9$. From these results and figure it is clear that in the presence of small uncertainty in the dynamic system, the proposed technique still results in a satisfactory performance which is due to the successful design procedure for the estimator.

TABLE II

RSSES COMPUTED FOR THE CASES OF WITHOUT THE PROCESS NOISE AND WITH THE PROCESS NOISE FOR DIFFERENT α'S.

α	RSSE without the process noise	RSSE with the process noise
0.5	8.19	17.99
0.9	16.06	22.9
0.95	22.68	30.31

For comparison, we apply the proposed technique and the feedback linearization control technique of [20] (with the linearized

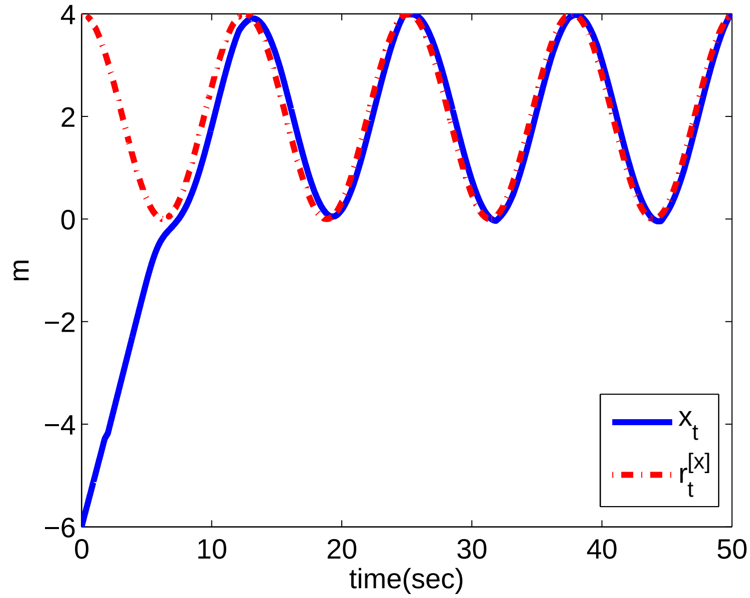

Fig. 5. Solid line: The x_t position of the autonomous vehicle. Dashed line: The desired position $r_t^{[x]}$ for the case, where the communication is subject to 90 percent packet drop out (i.e., $\alpha = 0.9$)

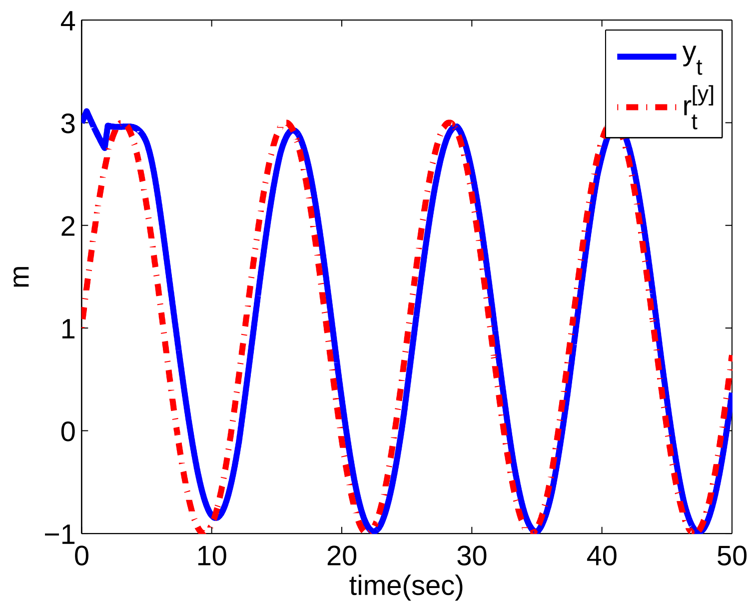

Fig. 6. Solid line: The y_t position of the autonomous vehicle. Dashed line: The desired position $r_t^{[y]}$ for the case, where the communication is subject to 90 percent packet dropout (i.e., $\alpha = 0.9$)

system of (9) and (10) of [20]) to the block diagram of Fig. 1 with the unicycle model of (21) as the dynamic system, with the reference signals $r_t^{[x]} = 0.05Tt$ and $r_t^{[y]} = 0.02Tt$ ($T = 0.01\,\text{sec}$) and the following initial conditions: x_0, $y_0 \in [-10, 10]$ and $\phi_0 \in [-2, 2]$. The RSSEs computed from the sample $t = 30/T$ to the sample $t = 100/T$ ($30\,\text{sec}$ to $100\,\text{sec}$) for $\alpha = 0.5$,

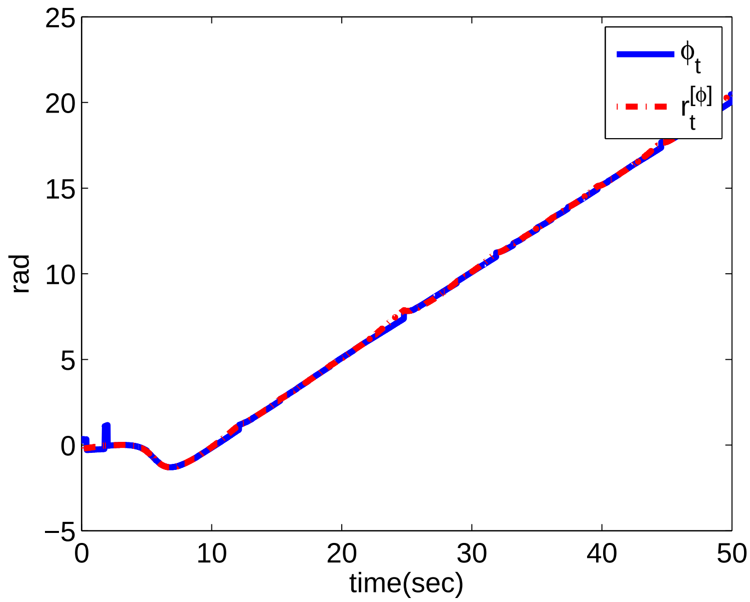

Fig. 7. Solid line: The orientation of the autonomous vehicle (ϕ_t). Dashed line: The desired orientation $r_t^{[\phi]}$ for the case, where the communication is subject to 90 percent packet dropout ($\alpha = 0.9$)

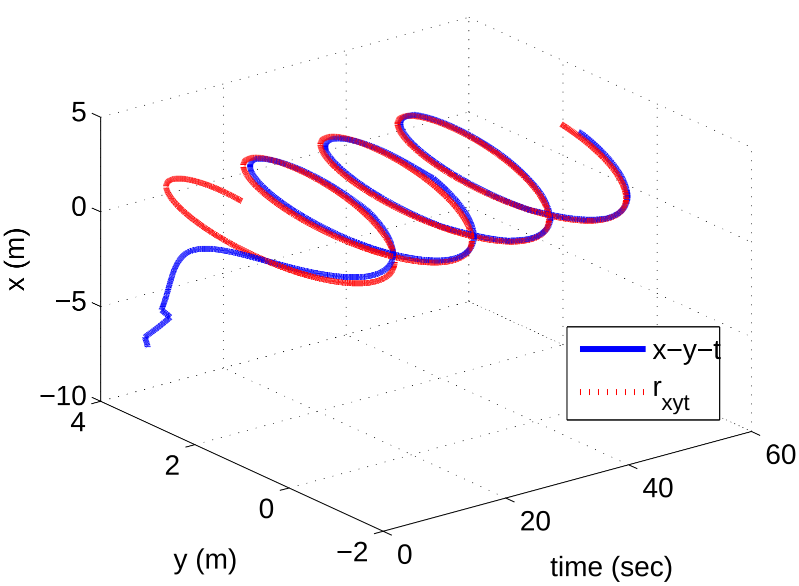

Fig. 8. $x_t - y_t - time$ diagram for the case where the communication is subject to 90 percent packet dropout ($\alpha = 0.9$). Solid line: $x_t - y_t - time$ diagram of the autonomous vehicle. Dashed line: The desired r_{xyt}

$\alpha = 0.9$ and $\alpha = 0.98$, when the proposed technique is used have been compared with those computed when the feedback linearization control technique of [20], is used in Table III. From these results and figures, it is clear that the proposed technique has much better performance.

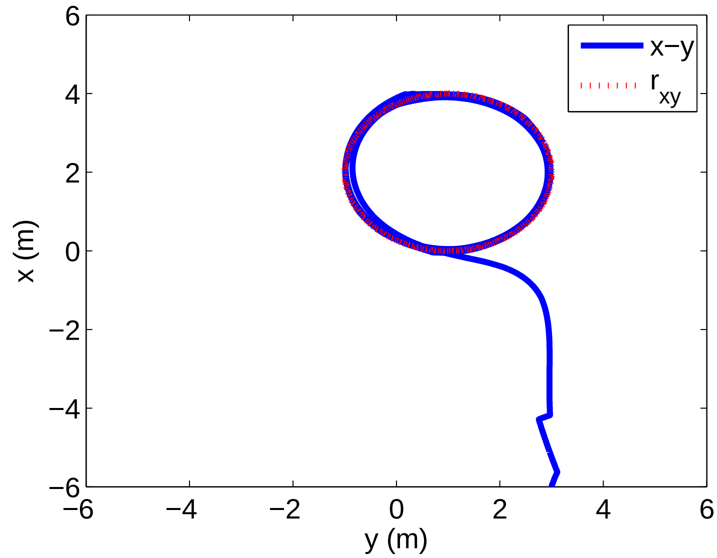

Fig. 9. $x_t - y_t$ diagram for the case where the communication is subject to 90 percent packet dropout ($\alpha = 0.9$). Solid line: $x_t - y_t$ of the autonomous vehicle. Dashed line: The desired r_{xy}

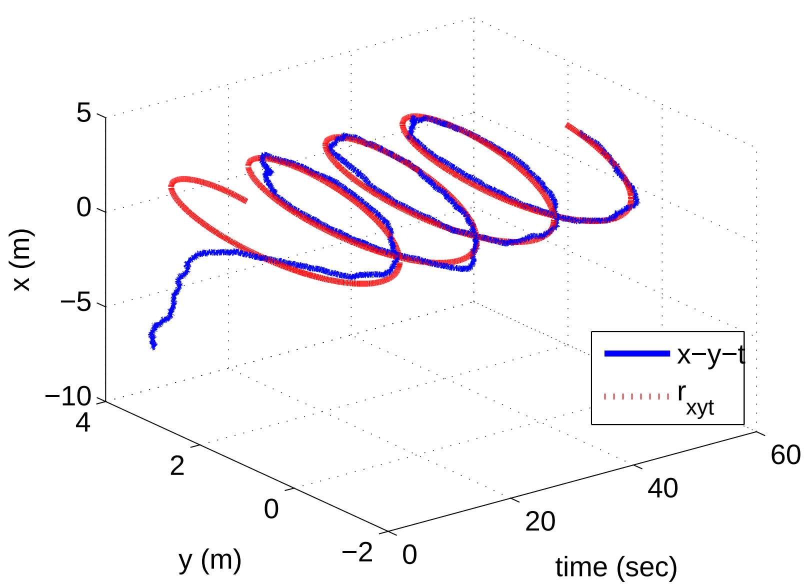

Fig. 10. $x_t - y_t - time$ diagram for the case where the communication is subject to 90 percent packet dropout ($\alpha = 0.9$) and the unicycle model is subject to process noise. Solid line: $x_t - y_t - time$ diagram of the autonomous vehicle. Dashed line: The desired r_{xyt}

Remark 4.1: In [18] the same dynamic system over the packet erasure channel with the erasure probability $\alpha = 0.5$, $\alpha = 0.9$ and $\alpha = 0.95$ is simulated and the obtained RSSEs are 1.21, 3.42 and 8.4, respectively (see Table IV). These indicate that using the technique of [18] by transmitting with less bits, a better performance is obtained. However, the technique of [18] requires

TABLE III

COMPARISON OF THE RSSEs COMPUTED FOR THE CASE WHEN THE PROPOSED TECHNIQUE IS USED WITH THOSE COMPUTED WHEN THE FEEDBACK LINEARIZATION CONTROL TECHNIQUE OF [20] IS USED.

α	RSSE for the proposed technique	RSSE for the other technique
0.5	1.98	30.23
0.9	2.86	230.75
0.98	6.44	617.14

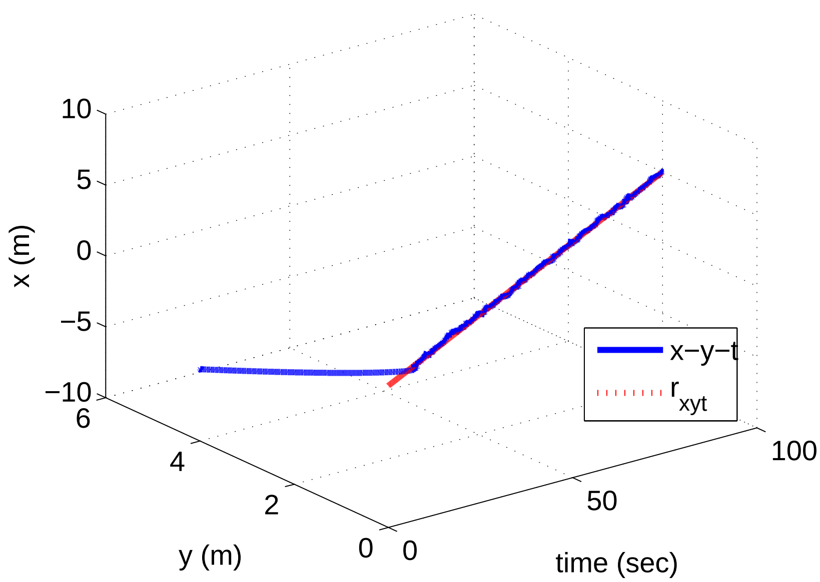

Fig. 11. $x_t - y_t - time$ diagram for the case of $\alpha = 0.9$ when the proposed technique is used for tracking a straight line

frequent linearization of the nonlinear system and transmission with variable bit rates, in which it may not be implementable for some dynamics (e.g., fast dynamics). That is, the proposed nonlinear coding and controller in this paper can be implemented with a fixed bit rate to a larger class of nonlinear systems including systems with uncertainty.

TABLE IV

COMPARISON OF THE RSSEs COMPUTED FOR THE CASE WHEN THE PROPOSED TECHNIQUE IS USED WITH THOSE COMPUTED WHEN THE TECHNIQUE OF [18] IS USED.

α	RSSE for the proposed technique	RSSE for the technique of [18]
0.5	8.19	1.21
0.9	16.06	3.42
0.95	22.63	8.4

Up to now, we have set the sample period to be $T = 0.01$ seconds. Now, we study the effects of the sampling period on the performance of the proposed technique. In order to address this question, we repeat simulations for different α's and

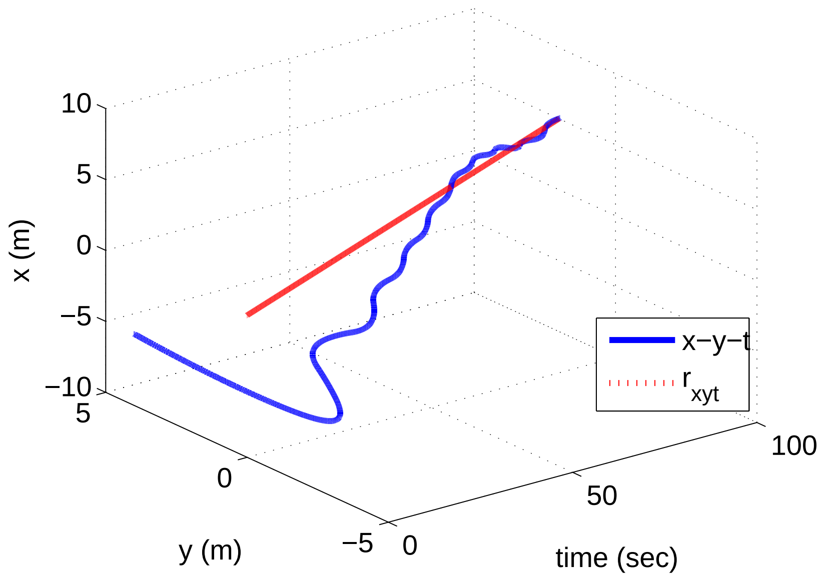

Fig. 12. $x_t - y_t - time$ diagram for the case of $\alpha = 0.9$ when the feedback linearization technique of [20] is used for tracking a straight line

different sampling periods. Table V summarizes the simulation results by presenting the corresponding RSSEs computed from the sample t = 30/T to the sample t = 50/T (30 sec. to 50 sec.) for $\alpha = 0.5$, $\alpha = 0.9$ and $\alpha = 0.95$ and $T = 0.001$, $T = 0.01$and $T = 0.1$. Note that the number of sample points that are used for the computation of RSSE for the case of $T = 0.001$ is 10 times larger than that of used for $T = 0.01$. Similarly, the number of sample points that are used for the computation of RSSE for the case of $T = 0.01$ is 10 times larger than that of used for $T = 0.1$. Therefore, in order to have a fair comparison between RSSEs for different sampling periods, we need to normalized RSSEs for the cases of $T = 0.001$ and $T = 0.1$ by multiplying them by $\sqrt{0.1}$ and $\sqrt{10}$, respectively. From Table V it follows that, as it is expected, by increasing the sampling period, the control performance is deteriorated. This is expected because for very small sample period (e.g., $T = 0.001$ and $T = 0.01$) the equivalent discrete time model that is used for designing controller, is a good approximation of the continuous time system. As it is clear from Table V, this deterioration in performance, which is due to the large sample period, is more obvious for larger α's, as it is seen in Fig. 13.

TABLE V

COMPARISON OF THE RSSES COMPUTED FOR DIFFERENT SAMPLE PERIODS T AND α.

α	T	RSSE	RSSE normalized	α	T	RSSE	α	T	RSSE	RSSE normalized
0.5	0.001	26.6284	8.42	0.5	0.01	8.19	0.5	0.1	5.6531	17.876
0.9	0.001	27.1614	8.58	0.9	0.01	16.06	0.9	0.1	10.546	33.34
0.95	0.001	28.9275	9.14	0.95	0.01	22.68	0.95	0.1	23.843	75.39

Remark 4.2: From Table I it follows that the proposed techniques are able to provide reliable real time estimation and a satisfactory reference tracking performance even for those α's that are close to one (i.e., for the cases subject to almost 100 percent packet dropout). But, in order to have this satisfactory performance, we need to allocate a very large transmission rate, where as α converges to one, this rate significantly rises. From Table II it follows that the proposed technique also provides a satisfactory performance in the presence of model uncertainty; and from Table V it follows that the proposed technique may not result in a satisfactory performance for large sampling periods.

V. Conclusion and Direction for Future Research

This paper presented a new technique for state estimation and reference tracking of nonlinear dynamic systems by a remote controller over the packet erasure channel. A new encoder and decoder for the state estimation of nonlinear dynamic systems at the end of communication link, were presented when measurements were sent through the packet erasure channel. Then, using the classical control theory tools, a controller for reference tracking of the system was also designed. That is, for nonlinear dynamic systems, almost sure asymptotic state estimation and reference tracking techniques including an encoder, decoder and a controller were presented. The satisfactory performances of the proposed state estimation and reference tracking techniques were illustrated via computer simulations by applying these techniques on the unicycle model, which represents the dynamics of autonomous vehicles. Since we have considered the effects of communication imperfections (random packet dropout and limited bit rate); and we compensated these imperfections in our theoretical development, a tele-operated system that is developed based on the results of this paper will have a larger operating range with an increased on-bored battery life time compared with the available IoT - based tele-operated systems.

For future it is interesting to extend the results of this paper to partially observed noisy nonlinear dynamic systems. For future, it is also interesting to combine our coding scheme with the coding-decoding based protocols (e.g., [21]) and event triggering protocols (e.g., [22]). Also, it is interesting to consider constraints on state variables and control inputs or consider prescribed performance. The methodologies used in [23] and [24] can be used to address this important extension. The technique proposed in this paper is perhaps applicable to the tele-operation of other robotic systems, e.g., manipulators and satellites. Addressing this question is also left for future investigation.

References

[1] S. Tatikonda and S. Mitter: 'Control over noisy channels', IEEE Transactions on Automatic Control, 2004, 49(7), pp. 1196-1201.

[2] A. Farhadi: ' Feedback channel in linear noiseless dynamic systems controlled over the packet erasure network', International Journal of Control, 88(8), 2015, 1490-1503.

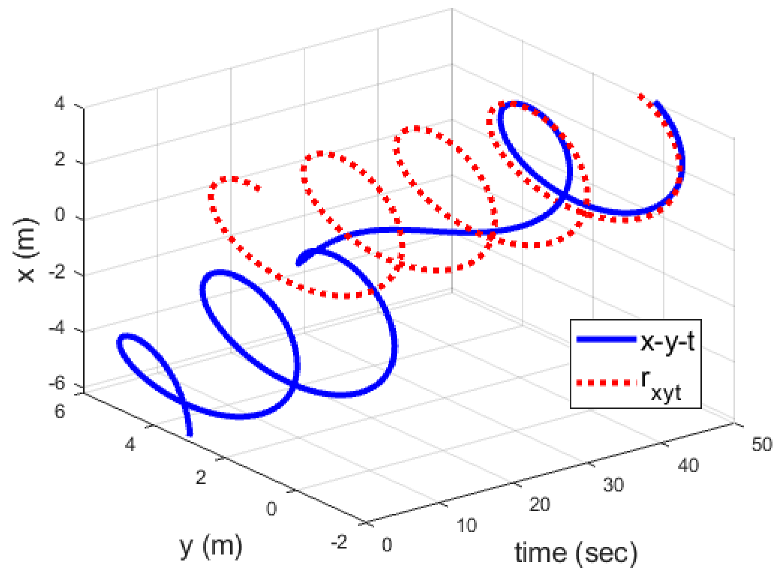

Fig. 13. $x_t - y_t - time$ diagram for the case of $\alpha = 0.95$ and $T = 0.1$

[3] A. Farhadi, and C. D. Charalambous: ‘ Stability and reliable data reconstruction of uncertain dynamic systems over finite capacity channels’, Automatica, 46(5), 2010, 889-896.

[4] A. Farhadi: ‘Stability of linear dynamic systems over the packet erasure channel: a co-design approach’, International Journal of Control, 2015, 88(12), pp. 2488-2498.

[5] C. D. Charalambous, A. Farhadi, S. Z. Denic: ‘Control of continuous-time linear Gaussian systems over additive Gaussian wireless fading channels: a separation principle’, IEEE Transactions on Automatatic Control, 2008, 53(4), pp. 1013-1019.

[6] N. C. Martins, A. Dahleh and N. Elia: ‘Feedback stabilization of uncertain systems in the presence of a direct link’, IEEE Transactions on Automatatic Control, 2006, 51(3), pp. 438-447.

[7] G. N. Nair, R. J. Evans, I. M. Y. Mareels and W. Moran: ‘Topological feedback entropy and nonlinear stabilization’, IEEE Transactions on Automatatic Control, 2004, 49(9), pp. 1585-1597.

[8] G. Fettweis and S. Alamouti: ‘5G: personal mobile Internet beyond what cellular did to telephony’, IEEE Communications Magazine, 2014, 52(2), pp. 140-145.

[9] G. P. Fettweis: ‘The tactile Internet: applications and challenges’, IEEE Vehicular Technology Magazine, 2014, 9(1), pp. 64-70.

[10] N. Elia, and J. N. Eisenbeis: ‘ Limitations of linear control over packet drop networks’, IEEE Transactions on Automatic Control, 56(4), 2011, 826-841.

[11] A. Farhadi, J. Domun and C. Canudas de Wit: ‘A supervisory control policy over an acoustic communication network’, International Journal of Control, 2015, 88(5), pp. 946-958.

[12] W. P. M. H. Heemels, A. R. Teel, N. van de Wouw, D. Nesic: ‘ Networked control systems with communication constraints: tradeoffs between transmission intervals, delays and performance’, IEEE Transactions on Automatic Control, 2010, 55(8), pp. 1781 - 1796.

[13] U. Vaidya and N. Elia: ‘Limitation on nonlinear stabilization over erasure channels’, in Proceedings of the 49th IEEE Conference on Decision and Control, 2010, pp. 7551 - 7556.

[14] A. Diwadkar and U. Vaidya: ‘Limitations for nonlinear observation over erasure channel’, IEEE Transactions on Automatic Control, 2013, 58(2), pp.

454 - 459.

[15] L. Schenato, B. Sinopoli, M. Franceschetti, K. Poolla and S. Sastry: ‘Foundations of control and estimation over lossy networks’, Proceedings of the IEEE, 2007, 95(1), pp. 163 - 187.

[16] P. K. Mishra, D. Chatterjee and D. E. Quevedo: ‘Resource efficient stochastic predictive control over packet dropouts’, IET Control Theory and Applications, 2017, 11(11), pp. 1666 - 1673.

[17] V. Sanjaroon, A. Farhadi, A. S. Motahari and B. H. Khalaj: ‘Estimation of nonlinear dynamic systems over communication channels’, IEEE Transactions on Automatic Control, 2018, 63(9), pp. 3024 - 3031.

[18] A. Parsa and A. Farhadi: ‘Measurement and control of nonlinear dynamic systems over the internet (IOT): Applications in remote control of autonomous vehicles’, Automatica, 2018, 95, pp. 93 - 103.

[19] P. Billingsley: ‘Probability and Measure’, (John Wiley and Sons, 1995).

[20] G. Oriolo, A. De Luca and M. Vendittelli: ’WMR control via dynamic feedback linearization: design, implementation, and experimental validation’, IEEE Transactions on Control Systems Technology, 2002, 10(6), pp. 835-852.

[21] L. Wang, Z. Wang, G. Wei and F. E. Alsaadi: ’Synchronization control for a class of discrete-time dynamical networks with packet dropouts: a coding-decoding-based approach’, IEEE Transactions on Cybernetics, 2018, 48(8), pp. 2437 - 2448.

[22] L. Wang, Z. Wang, Q. Han and G. Wei: ’Finite-time state estimation for recurrent delayed neural networks with component-based event-triggering protocol’, IEEE Transactions on Neural Networks and Learning Systems, 2018, 29(4), pp. 1046 - 1057.

[23] K. Sun, S. Mou, J. Qiu, T. Wong and H. Gao: ’Adaptive fuzzy control for non-triangular structural stochastic switched nonlinear systems with full state constraints’,IEEE Transactions on Fuzzy Systems, 2019, 27(8), pp. 1587 - 1601.

[24] J. Qiu, K. Sun, I. J. Rudas and H. Gao, ’Command filter-based adaptive NN control for MIMO nonlinear systems with full state constraints and actuator hysteresis’, IEEE Transactions on Cybernetics, recently accepted article: doi: 10.1109/TCYB.2019.2944761